Research Article ISSN 2639-9466

Nanotechnology & Applications

Effect of Cadmium Sulfide Quantum Dots Capped with Dextrin on Erythrocyte *In Vitro*

Anahi Rodríguez-López[1], Jorge Reyes-Esparza[1], Gerardo González De la Cruz[2], Patricia Rodríguez-Fragoso[2], César Millán-Pacheco[1] and Lourdes Rodríguez-Fragoso[1*]

[1]*Facultad de Farmacia, Universidad Autónoma del Estado de Morelos, Cuernavaca 62210, Mexico.*

[2]*Departamento de Física, CINVESTAV - I.P.N. Apartado Postal 14-740, 07000, Ciudad de Mexico, México.*

[*]Correspondence:
Lourdes Rodríguez-Fragoso, M.D. and Ph.D., Av. Universidad 1001, Col. Chamilpa, Cuernavaca, Morelos, Mexico.

Received: 20 February 2020; **Accepted:** 15 March 2020

Citation: Anahi Rodríguez-López, Jorge Reyes-Esparza, Gerardo González De la Cruz, et al. Effect of Cadmium Sulfide Quantum Dots Capped with Dextrin on Erythrocyte *In Vitro*. Nano Tech Appl. 2020; 3(1): 1-8.

ABSTRACT

Erythrocytes are sensitive to the effects of interaction with external agents and pathogens, which results in biochemical and morphological changes. This study evaluated the effects of CdS-dextrin nanoparticles on the biocompatibility, morphology and ζ-potential of erythrocytes in vitro. Blood was obtained from healthy male Wistar rats and erythrocytes were obtained by centrifugation. Hemolysis and topographical analyses were done using spectrophotometry and AFM, respectively. Determination of ζ-potential and molecular docking were also performed. CdS-dextrin quantum dots were evaluated at 0.1, 1, 10, and 100 µg/mL. CdS-dextrin quantum dots produced hemolysis (5%) with all concentrations used. Morphological changes included loss of biconcavity, and surface cracks were observed with 0.1 and 1 µg/mL during 30 min of exposure. When erythrocytes were incubated for 60 minutes this resulted in loss of concavity, increased size, and the presence of surface accumulations, which increased in a concentration dependent manner. The ζ-potential values did not change, regardless of the concentration of quantum dots. The analysis of CdS-dextrin quantum dots uptake showed that they did not enter the cell, though green fluorescence surrounding the erythrocytes was observed. The molecular docking revealed that dextrin of quantum dots might be interacting with glucose transporter GLUT1. Therefore, the interaction of CdS-dextrin quantum dots with erythrocytes induce minimal hemolysis but important morphological changes. It is not clear if these changes could be associated with functional changes. These preliminary findings provide evidence that nanomaterials can interact with erythrocytes and might cause associated pathophysiological processes following human exposure.

Keywords

Erythrocytes, Cadmium sulfide, Hemolysis, ζ-potential, Quantum dots.

Introduction

The multiple advantages and biomedical applications of quantum dots (QDs) are well known nowadays [1,2]. However, their clinical use is still restricted because it has been shown they can be potentially toxic to humans. One of the great current challenges in nanomedicine is to produce small enough nanomaterials, capable of effectively entering the body and accessing the white site [3-5], but make them safe.

The use of quantum dots for theranostic purposes most often requires the intravascular route and, once they enter the bloodstream, they must contact all blood components. Erythrocytes are blood cells that are continually exposed to aggression during their life span, which results in constant biochemical and morphological changes [6-8]. While it has been reported that some nanomaterials are safe for these cells [9-11], it is well known that their interaction with nanomaterials has variegated effects depending on the nanomaterial employed. Some nanomaterials can induce hemolysis (immediate destruction of erythrocytes), which is dependent on the concentration and exposure time [12-14]. A nanoparticle can be prevented from producing hemolysis with surfactants [15] and coatings [16]. However, hemolysis is not the only alteration so far associated to nanomaterial/erythrocyte interaction. Some nanoparticles induce alterations that can lead to erythrocyte stress and their premature immediate death, which will trigger various pathophysiological effects associated with the

deficient compensation of erythropoiesis and the consecutive loss of its presence in the blood [17-20].

Our research group has evaluated CdS-dextrin QDs in recent years using different *in vitro* and *in vivo* models [21]. It has been previously reported that they can enter the cell and reach the nucleus. Experiments with animals report they can go through biological barriers, have important tissue delivery and can remain in tissues for prolonged periods of time after a single dose [22]. An important feature is that they are biocompatible and only produce organ-selective toxicity following administration for prolonged periods of time [23]. All these properties make them ideal for use with theragnostic purposes. However, because we have only assessed their intraperitoneal use in animal models, we do not know if they could interact with some blood components after coming into direct contact. Therefore, the aim of this study was to evaluated the effects of CdS-dextrin nanoparticles on biocompatibility, morphology and ζ-potential of erythrocytes *in vitro*.

Material and Methods

Reagents

The sodium chloride and potassium chloride reagents were obtained from Sigma Aldrich (St. Louis, MO). Phosphate-buffered saline (PBS) came from GIBCO® by life technologies™ (New York, USA). The cadmium sulfide quantum dots capped with dextrin were prepared according to previously reported procedure [21].

Animal handling and blood collection

Healthy male Wistar rats (20) were housed in light and temperature controlled (22 ± 1°C) rooms. They had free access to water and standard pellets (Rodent chow diet, USA) ad libitum. All experimental procedures followed the Institutional Guides for practice in animals and Welfare Act Public Laws of Morelos State (Mexico) and the Guide for the Care and Use of Laboratory Animals [24]. Animals were sacrificed under anesthesia, and then blood was drawn from the heart and collected in tubes with 3.2% sodium citrate (Becton Dickinson Co. New Jersey, USA). Erythrocytes were obtained according with the following method.

Preparation of erythrocytes

Erythrocytes were prepared following the method previously described by Nemmar et al. [25]. Briefly, the collected male Wistar rats' blood was mixed by inversion. Then, the erythrocytes were separated by centrifuging at 1000 rpm for 15 minutes. They were washed 4 times by suspending them in 0.9% NaCl, followed by centrifugation at 1200 g for 10 mins. Then, they were separated by centrifuging at 1000 rpm for 15 minutes. The resulting supernatant was collected for the hemolysis assay, topographical analysis, localization and determination of ζ-potential.

Hemolysis assay

The hemolytic assay used in the present study followed the method previously described by Neun and Dobrovolskaia, [26]. Briefly, for every assay, 1 x 10^7 erythrocytes were resuspended with KCl 150mM + Tris 3mM buffer and incubated with CdS-dextrin QDs at concentrations of 0.1, 1, 10, and 100 µg/mL. After 30 minutes of exposure, the supernatant was collected, transferred in a 96 well, and the amount of hemoglobin was measured at a wavelength of 550 nm in a spectrophotometer (Multimode Plate Reader VICTOR x3 PerkinElmer, Massachusetts, USA). For positive control we used NaCl 35mM buffer.

Topographical analysis of erythrocytes by AFM

Erythrocytes were prepared according to the above method. Cells were treated with CdS-dextrin QDs at different concentrations (0.1, 1, 10, and 100 µg/mL) and incubated again for 30 and 60 min. After this time, approximately 10 µL aliquots were taken and dry smears were performed on slides. An XE-Bio Atomic Force Microscope (Park Systems Co., Suwan, Korea) was used to obtain topographic images of the erythrocytes. We used XEP and XEI software from Park Systems to analyze the data. PPP-NCHR silicon nitride cantilevers with nominal spring constant of 42 N/m from nanosensors were used in non-contact mode. DNP-S-D silicon nitride cantilevers with nominal spring constant of 0.06 N/m (Bruker, USA) were used in Contact mode. The DNP-S-D cantilevers were calibrated using the Thermal Method routine built into the XEI software. Topographic representations were obtained at 21 ± 1°C. Images are 256 pixels x 256 pixels and were taken at a frequency between 1.5 and 3.5 Hz. Scans performed in Contact mode were carried out at load forces lower than 1 nN. The images shown correspond to one typical sample.

Determination of the zeta-potential (ζ-potential) in erythrocytes

The ζ-potential assay was performed using a Zetasizer Nano-ZS90 device (Malvern Instrument Inc., Westborough, USA). Isolated erythrocytes were washed and resuspended in 10% phosphate-buffer, pH 7.5. Cells were incubated and treated with CdS-dextrin QDs at different concentrations (0.1, 1, 10, and 100 µg/mL) during 30 min. Afterwards, ζ-potential was determined using a Zetasizer, which is based on the Lasser-Doppler microelectrophoresis technique [27]. ζ-potential was indirectly measured by monitoring particle speed using a laser, which enables the measuring of electrophoretic motility of erythrocytes. The results were analyzed using the Dispersion Technology Software 6.2 (Malvern Instrument Inc., Westborough, USA).

Fluorescent microscopic visualization of CdS-dextrin QDs in erythrocytes

The erythrocytes employed to verify selective uptake (1 x 10^7) were cultured for 10 min, washed with PBS and then incubated with CdS-dextrin QDs 0.1, 1, 10, 1 and 00 µg/mL during 30 min. The cells were seeded on slides by smearing and allowed to dry- Then they were placed above the objective on a confocal microscope. CdS-dextrin QDs were excited with a 488 nm laser, and their signals were collected from 515 nm. Slices were observed under fluorescence microscopy and analyzed using the Image-Pro Insight 9 software (Digital Imaging Systems, Bourne End, UK).

Molecular docking of interaction CdS-dextrin/erythrocyte

We used human glucose transporter GLUT1 (PDB ID: 4PYP) in

this study. GLUT1 was embedded on a membrane with 75/25 of 1,2-Dipalmitoylphosphatidylcholine (DPPC) and cholesterol, respectively. GLUT1 orientation followed the Orientations of Protein in Membrane (OPM) database [28]. The GLUT1 system was built using charmm-gui server [29]. Salt concentration was 0.15 M KCl. The complete system was equilibrated with Gromacs 2019.2 following inputs proposed by the charmm-gui server using charmm36 parameters. The last structure after equilibration was used as a receptor for docking studies We performed 50 independent blind docking runs of GLUT1 over the extracellular region (as reported on the OPM database) using Autodock vina 1.12 [30]. A grid box of 45x45x23Å with a 0.375 Å spacing was used. 6 and 12 dextrins were built using charmm-gui server by employing the glycan reader & model option. Both glycans were solvated and equilibrated with NAMD 2.12 using inputs provided by charmm-gui. Both systems were prepared on Pymol 2.3.0 using Autodock Vina. Plugin images were created by using Maestro [31] and VMD [32].

Statistical analysis

The data are represented as the mean ± SD of three different experiments. The data were processed by T-test (for independent groups) using SPSS 10.0 software (SPSS Inc., Chicago, IL, USA) software.

Results

Effect of CdS-dextrin QDs on the integrity of erythrocytes after 30 minutes of exposure

Figure 1 shows the effect of different concentrations (0.1, 1, 10, and 100 µg/mL) of CdS-dextrin QDs on the integrity of erythrocytes. Cells were incubated during 30 minutes with nanomaterial. It was observed that the CdS-dextrin QDs produced 5% hemolysis under all concentrations ($p<0.05$). These results indicate that CdS-dextrin QDs produce minimal lysis of erythrocytes.

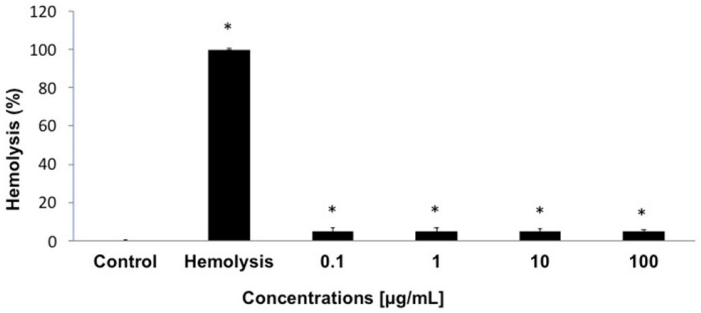

Figure 1: Effect of CdS/dextrin QDs on integrity of erythrocytes. Erythrocytes were treated with CdS-dextrin QDs at 0.1, 1, 10, and 100 µg/mL during 30 min. Control erythrocytes were considered as healthy cells not exposed to QD and hemolysis group were cells preincubated with NaCl 35mM. Results are expressed as the percentage of hemolysis as compared with hemolysis group. Data are presented as the mean ± SD of at least three independent experiment. * $p<0.05$ as compared with hemolysis group.

Effect of CdS-dextrin QDs on morphology and size of erythrocytes after 30 minutes of exposure

Figure 2 shows AFM images of erythrocytes treated with CdS-dextrin QDs during 30 and 60 min. The first two images correspond to untreated erythrocytes (control group) and erythrocytes treated with NaCl 35mM (hemolysis). First there is a 3D image of a healthy erythrocyte with oval morphology, biconcave with a central depression. Next to it is a hemolyzed erythrocyte. The cell shows a loss of its morphology due to the rupture of its membrane and the output of cellular content.

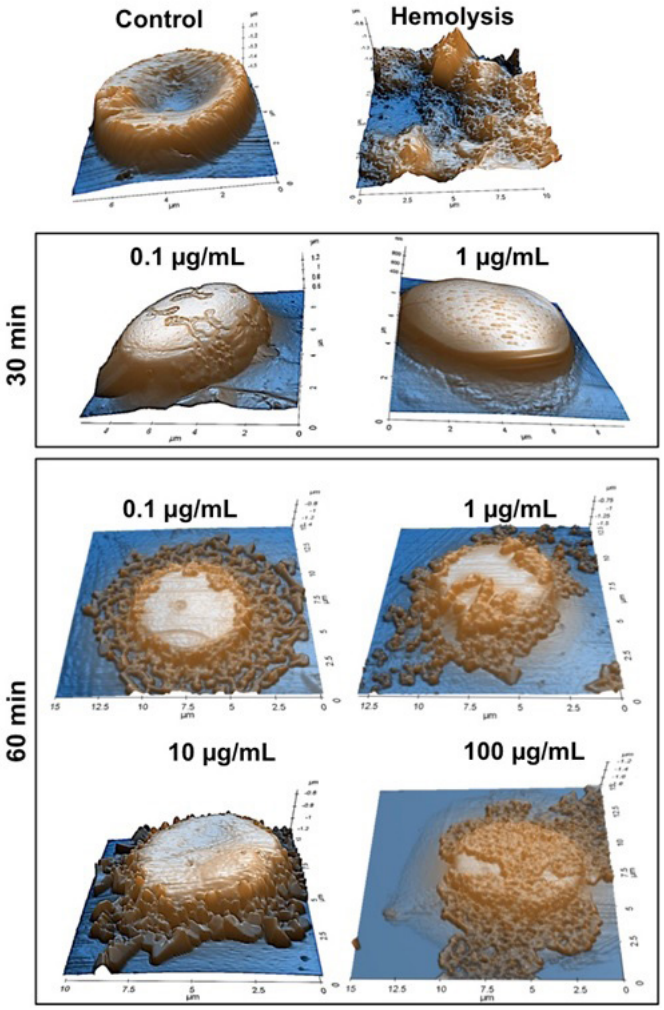

Figure 2: Representative AFM images showing the surface morphology of erythrocytes. Outer surface images were recorded in air tapping-mode AFM, images of typical circular, biconcave rat erythrocytes are shown in control group (height 3D image) and loss of morphology in hemolysis group. Erythrocytes treated with CdS-dextrin QDs at 0.1, and 1, µg/mL during 30 min showed alterations in their morphology. Erythrocytes treated with CdS-dextrin QDs at 0.1, 1, 10 and 100 µg/mL during 60 min showed loss of concavity, an apparent size increase, and the presence of surface accumulations. The image is representative of two experiments.

Erythrocytes treated with 0.1 µg/mL CdS-dextrin QDs during 30 min show a corpulent morphology and undefined edges, flat, with cracks on the surface and lacking a central depression, as shown in the 3D reconstruction. In the case of erythrocytes treated with 1 µg/mL of CdS QDs during 30 min, the cells showed defined and smooth edges, increased in width, flatness and lack of a central depression, as well as "artifacts" that made the surface

look rough, suggesting these could be nanoparticles (see image). Interestingly, erythrocytes treated with concentrations of 0.1, 1, 10, and 100 µg/mL during 60 min showed significant changes. The erythrocyte itself was intact and there was no rupture of its membrane, but there was a loss of concavity, an increased size, and the presence of surface accumulations, which increased alongside QD concentration. Although the hemolysis analysis revealed 5% of it, the AFM analysis showed no evidence of hemolysis with any QD concentration. This discrepancy in the results may indicate that the observed hemolysis might be due to sample manipulation. Interestingly, a topographical analysis showed loss of biconcavity in those erythrocytes treated with CdS-dextrin QDs. However, there was no increase in the size of erythrocytes at any concentration oe under any time of exposure (see ΔX values, Figure 3).

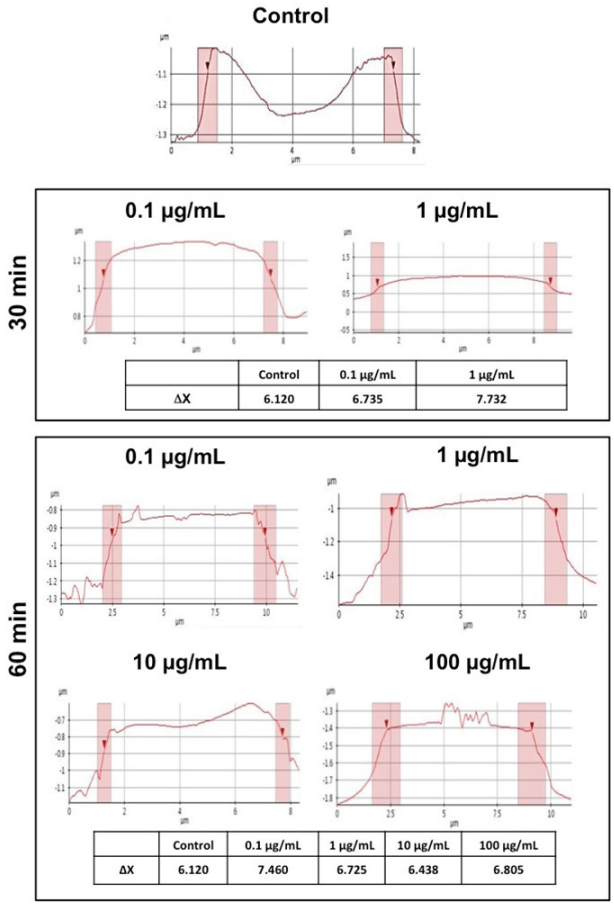

Figure 3: Topographic height-AFM images of erythrocytes treated with CdS-dextrin QDs at 0.1 and 1µg/mL during 30 min or 0.1, 1, 10 and 100 µg/mL during 60 min. ΔX shows that the size of erythrocytes did not change regardless of QD concentration and exposure time. The image is representative of two experiments.

Determination of the ζ -potential in erythrocytes treated with CdS-dextrin QDs as a measure of cell membrane integrity

In Figure 4, we can see the ζ-potential recorded in healthy erythrocytes and erythrocytes treated with CdS-dextrin QDs. The net ζ-potential on cell membrane of live cells is determined, among other factors, by the organization and intermolecular interactions of its components (proteins and lipids). In erythrocytes treated with concentrations of 0.1 to 100 µg/mL, ζ-potential was close to the control values- That is, it was indicative of the fact that the CdS-dextrin QDs did not affect the ζ-potential of the erythrocyte membranes.

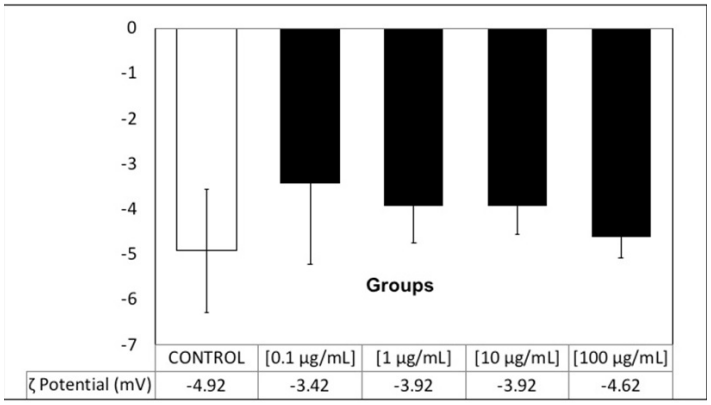

Figure 4: The zeta potential of erythrocytes after exposure to CdS/dextrin QDs. Healthy erythrocytes were taken as the control group. Erythrocytes were treated with CdS/dextrin QDs at 0.1, 1, 10 and 100 µg/mL during 30 min. ζ -potential of erythrocytes was detected in independent duplicates. Data are presented as the mean ± SD. * $p<0.05$ as compared with control group.

In vitro cellular uptake and localization of CdS-dextrin QDs in erythrocytes

Erythrocytes were incubated with 0.1, 1, 10, and 100 µg/mL of CdS-dextrin QDs for 30 min and then washed to remove any unbound nanoparticles (Figure 5). Untreated erythrocytes showed the usual morphology for these cells, including the presence of biconcave morphology. There was no fluorescence detected inside of cells. Erythrocytes treated with 0.1 and 1 µg/mL CdS-dextrin QDs showed minimal fluorescence, and there was no clear uptake by the cells. Interestingly, erythrocytes treated with 10 and 100 µg/mL showed green fluorescence surrounding them; this increased alongside the concentration of quantum dots. These findings show that, at times, erythrocytes were unable to uptake CdS-dextrin QDs.

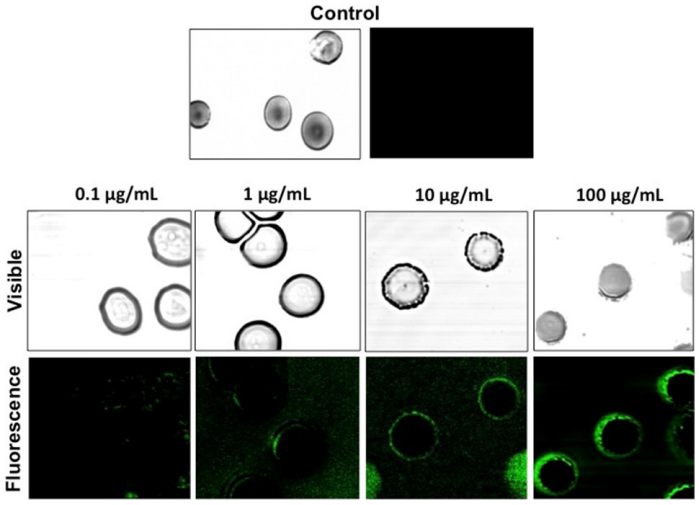

Figure 5: Fluorescent microscopic visualization of CdS/dextrin QDs in erythrocytes. Erythrocytes were treated for 30 min with CdS/dextrin QDs (0.1 – 100 µg/mL). Cells were seeded on slides by smearing and allowed

to dry, then analyzed using confocal epifluorescence microscope. Green fluorescence shows the presence of QDs surrounding the erythrocytes.

Molecular docking of CdS-dextrin/erythrocyte

A hypothetical system was created to get a possible binding mode between CdS spheres covered with dextrins and the main protein on the erythrocyte membrane, glucose transporter GLUT1. Due to the lack of molecular structures of CdS spheres with dextrins, only one dextrin of each size was docked with GLUT1 transporter. 50 independent docking runs were performed using the GLUT1 structure and two dextrins of different size: 6 and 12 sugars (Figure 6A panel). Dextrins were docked on the same region of GLUT1 transporter (Figure 6 B and C panels). GLUT1 residues involved in the potential binding site of dextrins reported by autodock vina were: 37, 38, 41, 58, 61, 62, 65, 66, 296, 299 to 304, 355 to 366, 423, 424, 426 to 432 (residue numbers as on the original PDB).

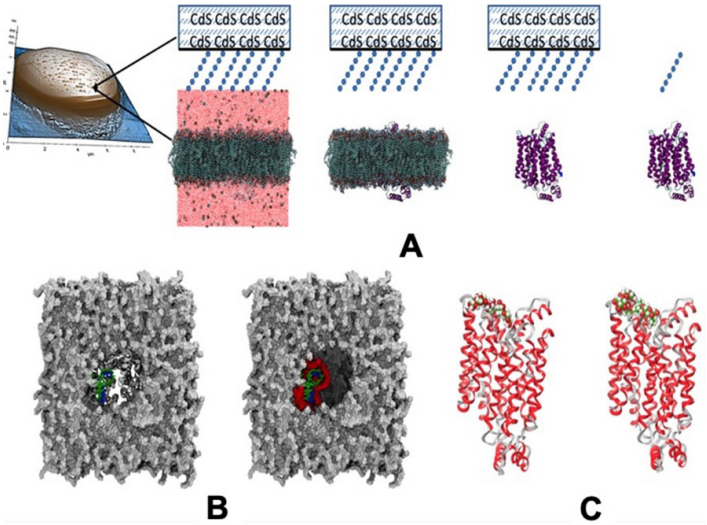

Figure 6: Hypothetical glucose transporter GLUT1 bound to dextrins. A) Schematic representation of the procedure used on this work. B) Membrane molecular surface with one representative structure of both dextrins (6 sugars on blue sticks and 12 sugars on green sticks) with GLUT1 on the center of the image. Most of the docking results bound to one side of GLUT1 surface (in red). C) GLUT 1 cartoon representation with 6 and 12 sugars (left and right, respectively).

Discussion

QD applications have increased in recent years. However, even with their potential utility, their toxicity is still closely associated with size, composition, loading and coating, among other characteristics. Here we evaluate the *in vitro* effects of the interaction of CdS-dextrin QDs with rat erythrocytes and show that CdS-dextrin QDs may cause important morphological changes without modifying the ζ-potential in the erythrocyte and or inducing cell death.

Previous studies have shown that the exposure of erythrocytes to QDs is associated with toxicity [32,33]. Gold nanoparticles of 30 nm in size produced hemolysis, and no such effect was observed with smaller nanoparticles (5.10, 20 nm) [34]. Contrary to the above, another study with silver nanoparticles showed that smaller nanoparticles (1-3 nm) produced greater hemolytic activity (60%) [35], suggesting that hemolysis induction is independent of size. Likewise, 3.2 nm gold nanoparticles coated with polyethylene glycol produced minimal hemolysis (<5%) with concentrations of 100 µg/mL, but nanoparticles not coated produced greater hemolysis (70%) at concentrations of 30 µg/mL [36]. Reports from other studies using QDs coated with different materials or drugs have shown a reduction in the hemolytic effect [37,38] suggesting that size and coating could help reduce the hemolytic effect of certain nanomaterials. In the present work the erythrocytes were exposed to CdS-dextrin QDs for 30 min and we observed minimal hemolysis (<5%), even at the concentration of 100 µg/mL. The nanoparticles used in the present study have the characteristic of being small in size (3-5 nm) and are also coated with dextrin. Which suggests that as with nanomaterials, the small size and dextrin coating could be protecting the core of CdS and thus be more biocompatible with erythrocytes.

It is suggested that erythrocytes are cells sensitive to the effect of some nanomaterials and as a result of such interaction membrane and morphological alterations of the erythrocyte can occur [39]. It has been reported that TiO_2 nanoparticles of a size of 20 and 200 nm, produced deformation of the erythrocyte membrane at a concentration of 100 µg/mL, the effect being more marked with those of smaller size [40]. In another study, it was reported that erythrocytes treated with SiO_2 nanoparticles of a size of 30 nm at a concentration of 1 mg/mL produced morphological alterations and adhesion of erythrocytes; while erythrocytes treated with ZrO_2 nanoparticles (80-100 nm) and Al_2O_3 nanoparticles (15-60 nm) at a concentration of 2 mg/mL produced surface cracks and the biconcavity was lost. Additionally, erythrocytes treated with Al_2O_3 presented vesicles on the erythrocyte membrane and the changes produced were irreversible [41]. In our study, we observed that erythrocytes treated with CdS-dextrin QDs (3-5 nm) caused morphological changes in the erythrocyte membrane at concentrations of 0.1 and 1 µg/mL after 30 min of exposure. The alterations that were observed were loss of biconcavity, cracks and small lumps on the surface of the membrane. However, in the erythrocytes treated for 60 minutes, in addition to the aforementioned alterations, it was observed that there was an agglomeration of the nanoparticles on the cell surface with all the concentrations studied. The AFM images and topographic measurements showed evidence that CdS-dextrin QDs produced morphological alterations similar to those already reported, given their small size they could have a larger surface area to interact with the erythrocyte membrane.

The charge of the cell membrane depends directly on the composition of the cell membrane and the physiological state of the cell, so changes in the ζ-potential may reflect morphological and/or functional changes [42,43]. Changes in the ζ-potential of membrane have been associated by the presence of certain materials in some cells, including erythrocytes. As demonstrated in the study by Bondar et al., [44] where the effect of different polymers on the ζ-potential in cervical adenocarcinoma cells (HeLa), breast adenocarcinoma (MCF-7) and erythrocytes was evaluated, as a

biophysical indicative of the physiological composition of cells. It was shown that the interaction of the cells with poly-L-lysine (20 µg/mL) and polyethyleneimine (5 µg/mL) modified the ζ-potential of the cell membrane towards positivity which was associated with a reduction in viability and presence of apoptosis. On the other hand, it has been observed that erythrocytes exposed to nanocapsules of glycerol monolaurate did not induce toxicity and this correlated with no changes in the ζ-potential of the erythrocyte [45]. Our results showed that the exposure of erythrocytes with CdS-dextrin QDs at concentrations of 0.01 to 100 µg/mL for 30 minutes did not produce changes in ζ-potential. Although we observe morphological changes of the erythrocyte, there are probably no changes in membrane integrity. Therefore, based on other studies we can suggest that the interaction of the CdS-dextrin QDs/erythrocytes probably does not affect the functionality, since we do not observe changes in the net charge of the cell surface, at least a short exposure time.

Previous studies with CdS-dextrin QDs have been shown to be easily internalized and distributed homogeneously inside non-blood cells, and that uptake has been dose-dependent manner [22]. It is known that there are nanomaterials that cannot reach the cell nucleus, such is the case of carboxylated QDs (625 nm) that were evaluated in human bone marrow cells for 1, 3, 6 and 24 hours, where it was shown that QDs were easily internalized but were located only in the cytoplasm and on the cell surface, without reaching the nucleus [46]. The erythrocytes have been used for the delivery of contrast agents through the use of magnetic nanoparticles, the above has been achieved through the temporary opening of pores in the erythrocyte membrane so that they can cross the nanoparticles and can remain within these cells a once the pores close [47]. This methodology has proved to be stable, versatile, safe and easy to manufacture. However, there are no reports indicating that erythrocytes are capable of internalizing nanomaterials by themselves. In this study, the ability of the erythrocyte to capture CdS-dextrin QDs was evaluated using concentrations of 0.1 to 100 µg/mL, after exposure for 30 min. By confocal microscopy it was possible to observe that QDs only surrounded the erythrocytes, that is, the erythrocyte was unable to internalize CdS-dextrin QDs. These findings correlated with the AFM studies, where it was shown that QDs remained on the cell surface. It has been reported that a cell internalizes nanoparticles through active internalization mechanisms: endocytosis, macropinocytosis, phagocytosis and pinocytosis (this being the most common). These mechanisms encapsulate NPs in selectively transported vesicles, and it is estimated that size, surface charge of NPs, as well as transport machinery [48] are involved in each mechanism. However, it is known that erythrocyte does not have endocytosis mechanisms or active transport due to its limited metabolism, perhaps that may be the reason why it cannot internalize QDs.

The molecular docking analysis suggests that changes in the shape of the erythrocyte may be due to molecular interactions between the dextrin that covers the core of CdS and the cell surface. The schematic representation obtained from molecular docking shows that dextrin can bind to the GLUT1 glucose transporter. As Galochkina et al show, the salt bridge formed by residues K38 and E299 are key to glucose absorption [49]. Our coupling results can give an explanation to the morphological changes of the erythrocytes since the interaction of dextrin can alter the natural conformational movement of the GLUT1 transporter, and with this produce a decrease in glucose absorption. Although the potential ζ did not show changes in the erythrocyte that could indicate a functional change thereof, by AFM techniques it was shown that the QDs do remain on the cell surface and are associated with a morphological change of the cell. Therefore, the molecular docking analysis suggests that there could be modifications in important components of the cell membrane that lead to functional changes of the erythrocyte.

Conclusion

The results showed that the CdS-dextrin QDs produce minimal hemolysis but induce notable morphological changes of erythrocytes. However, it is not clear whether these changes could be associated with functional changes. Therefore, further studies are necessary to clarify this matter and assess whether the interaction of the CdS-dextrin QDs/erythrocyte can trigger associated pathophysiological effects *in vivo*.

Acknowledgements

The authors are grateful to M. Sci. Arturo Galvan Hernández at Institute of Physical Science (UNAM) for his technical assistance in obtaining AFM images and to Q.F.B Xochitl Alvarado Affantrager at the National Laboratory of Advanced Microscopy (UNAM) for her technical assistance in obtaining confocal microscopy images.

References

1. Volkov Y. Quantum dot in nanomedicine: recent trends, advances and unresolved issues. Biochem Biophys Res Commun. 2015; 468: 419-427.
2. Devi P, Saini S, Kim KH. The advanced role of carbon quantum dots in nanomedical applications. Biosens Bioelectron. 2019: 141: 111158.
3. Huang H, Lovell JF. Advanced Functional Nanomaterials for Theranostics. Adv Funct Mater. 2017: 27.
4. Mitragotri S, Anderson DG, Chen X, et al. Accelerating the Translation of Nanomaterials in Biomedicine. ACS Nano. 2015: 9: 6644-6654.
5. Nag OK, Delehanty JB. Active Cellular and Subcellular Targeting of Nanoparticles for Drug Delivery. Pharmaceutics. 2019: 11: 543-543.
6. Ahmad IZ, Kuddus M, Tabassum H, et al. Advancements in Applications of Surface Modified Nanomaterials for Cancer Theranostics. Curr Drug Metab. 2017: 18: 983-999.
7. Cluitmans JCA, Chokkalingam V, Janssen AM, et al. Alterations in Red Blood Cell Deformability during Storage: A Microfluidic Approach. Biomed Res Int. 2014: 764268.
8. Schaeffer EK, West RJ, Conine SJ, et al. Multiple physical stresses induce γ-globin gene expression and fetal hemoglobin production in erythroid cells. Blood Cells Mol Dis. 2014: 52: 214-224.

9. Zhang H. Erythrocytes in nanomedicine: an optimal blend of natural and synthetic materials. Biomaterials. Sci. 2016: 4: 1024-1031.
10. Kim J, Heo YJ, Shin S. Haemocompatibility evaluation of silica nanomaterials using hemorheological measurements. Clin Hemorheol Microcirc. 2016: 62: 99-107.
11. Li S, Guo Z, Zhang Y, et al. Blood Compatibility Evaluations of Fluorescent Carbon Dots. ACS Appl Mater Interfaces. 2015: 7: 19153-19162.
12. Barshtein G, Livshits L, Shvartsman LD, et al. Polystyrene Nanoparticles Activate Erythrocyte Aggregation and Adhesion to Endothelial Cells. Cell Biochem Biophys. 2016: 74: 19-27.
13. Ekstrand-Hammarström B, Hong J, Davoodpour P, et al. TiO_2 nanoparticles tested in a novel screening whole human blood model of toxicity trigger adverse activation of the kallikrein system at low concentrations. Biomaterials. 2015: 51: 58-68.
14. Zeng H, Changjian L, Zhang X, et al. The effects of gold nanoparticles on the human blood functions. Artif Cells Nanomed Biotechnol. 2018: 46: 720-726.
15. Chen LQ, Fang L, Ling J, et al. Nanotoxicity of Silver Nanoparticles to Red Blood Cells: Size Dependent Adsorption, Uptake, and Hemolytic Activity. Chem Res Toxicol. 2015: 28: 501-509.
16. Thasneem YM, Sajeesh S, Sharma CP. Effect of thiol functionalization on the h6mo-compatibility of PLGA nanoparticles. J Biomed Mater Res. 2011: 99: 607-617.
17. Ran Q, Xiang Y, Liu Y, et al. Eryptosis Indices as a Novel Predictive Parameter for Biocompatibility of Fe3O4 Magnetic Nanoparticles on Erythrocytes. Sci Rep. 2015: 5: 16209.
18. Ferdous Z, Beegam S, Tariq S, et al. The *in Vitro* Effect of Polyvinylpyrrolidone and Citrate Coated Silver Nanoparticles on Erythrocytic Oxidative Damage and Eryptosis. Cell Physiol Biochem. 2018: 49: 1577-1588.
19. Lang E, Lang F. Mechanisms and pathophysiological significance of eryptosis, the suicidal erythrocyte death. Semin Cell Dev Biol. 2015: 39: 35-42.
20. Lang KS, Lang PA, Bauer C, et al. Mechanisms of suicidal erythrocyte death. Cell Physiol Biochem. 2015: 15: 195-202.
21. Jorge Reyes-Esparza, Alberto Martínez-Mena, Ivonne Gutiérrez-Sancha, et al. Synthesis, characterization and biocompatibility of cadmium sulfide nanoparticles capped with dextrin for *in vivo* and *in vitro* imaging application. J Nanobiotechnology. 2015: 13: 2-14.
22. Gerardo Gonzalez De La Cruz, Rocío Gómez-Cansino1, Patricia Rodríguez-Fragoso, et al. Disposition and Biocompatibility of Dextrin-coated cadmiun sulfhide nanoparticles after a single dose and multiple doses in rats. Indian J Pharm Sci. 2019: 81: 876-884.
23. Gómez-Cansino R, Rodríguez-Fragoso L. Long Exposure to CdS-Dextrin Nanoparticles Induces an Immunomodulatory and Anti-Inflammatory Effect in Rats. J Mater Sci Nanotechnol. 2017: 5: 105.
24. https://grants.nih.gov/grants/olaw/Guide-for-the-care-and-use-of-laboratory-animals.pdf.
25. Nemmar A, Zia S, Subramaniyan D, et al. Interaction of diesel exhaust particles with human, rat and mouse erythrocytes *in vitro*. Cell Physiol Biochem. 2012: 29: 163-170.
26. Neun B, Dobrovolskaia MA. Method for analysis of nanoparticle hemolytic properties *in vitro*. Nano Lett. 2011: 697: 215-224.
27. Tokumasu F, Nardone GA, Ostera GR, et al. Altered membrane structure and surface potential in homozygous hemoglobin C erythrocytes. PLoS One. 2009: 4: e5828.
28. Lomize MA, Pogozheva ID, Lomize AL, et al. OPM database and PPM web server: Resources for positioning of proteins in membranes. Nucleic Acids Res. 2012: 40: 370-376.
29. Wu EL, Dávila-Contreras EM, Im W. CHARMM-GUI Membrane Builder toward realistic biological membrane simulations. J Comput Chem. 2014: 35: 1997-2004.
30. Jing Huang, Alexander D MacKerell Jr. CHARMM36 all-atom additive protein force field: Validation based on comparison to NMR data. J Comput Chem. 2013: 34: 2135–2145.
31. Trott O, Olson AJ. AutoDock Vina: Improving the speed and accuracy of docking with a new scoring function, efficient optimization, and multithreading. J Comput Chem. 2010: 31: 455-461.
32. Sang-Jun Park, Jumin Lee, Dhilon S Patel, et al. Glycan Reader is improved to recognize most sugar types and chemical modifications in the Protein Data Bank. Bioinformatics. 2017: 33: 3051-3057.
33. A Tsatsakis, A K Stratidakis, A V Goryachaya, et al. *In vitro* blood compatibility and *in vitro* cytotoxicity of amphiphilic poly-Nvinylpyrrolidone nanoparticles. Food Chem Toxicol. 2019: 127: 42-52.
34. Cenni E, Baldini N. Biocompatibility of poly (D,L-lactide-co-glycolide) nanoparticles conjugated with alendronate. Biomaterials. 2008: 29: 1400-1411.
35. Aseichev A, Sergienko VI. Effects of Gold Nanoparticles on Erythrocyte Hemolysis. Bull Exp Biol Med. 2014: 156: 495-498.
36. Barrios-Gumiela A, Gómez R, De la Mata J, et al. Effect of PEGylation on the biological properties of cationic carbosilane dendronized gold nanoparticles. Int J Pharm. 2020: 573: 118867.
37. Sun C, Lee J, Zhang M. Magnetic nanoparticles in MR imaging and drug delivery. Adv Drug Deliv Rev. 2008: 60: 1252-1265.
38. SN Pleskova, EE Pudovkina, ER, ER Mikheeva, et al. Interactions. Interactions of Quantum Dots with Donor Blood Erythrocytes *In Vitro*. Bull Exp Biol Med. 2014: 156: 384-388.
39. Chen YC, Hsieh WY, Lee WF, et al. Effects of surface modification of PLGA-PEG-PLGA nanoparticles on loperamide delivery efficiency across the blood–brain barrier. J Biomater Appl. 2011: 27: 909-922.
40. Pretorius E, Du Plooy JN, Bester J. A Comprehensive Review on Eryptosis. Cell Physiol Biochem. 2016: 39: 1977-2000.
41. Shi-Qiang L, Rong-Rong Z, Hong Z, et al. Nanotoxicity of TiO_2 nanoparticles to erythrocyte *in vitro*. Food and Chem Toxicol. 2008; 46: 3626-3631.
42. Kozelskaya AI, Vasyukov Y, AV Panin, et al. Morphological changes of the red blood cells treated with metal oxide

nanoparticles. Toxicol *in Vitro*. 2016: 37: 34-40.
43. Furusawa K, Uchiyama K. Collaborative studies of zeta-potential measurements and electrophoretic measurements using reference sample. Colloids Surfaces A: Physicochem Eng Aspects. 1998: 140: 217-226.
44. Mokrushnikov PV, Panin LE, Zaitsev BN. The action of stress hormones on the structure and function of erythrocyte membrane. Gen Physiol Biophys. 2015: 34: 311-321.
45. Bondar OV, Saifullina DV, Shakhmaeva II, et al. Monitoring of the Zeta Potential of Human Cells upon Reduction in Their Viability and Interaction with Polymers. Acta Naturae. 2012: 4: 78-81.
46. Agulla J, Brea D, Argibay B, et al. Quick adjustment of imaging tracer payload, for *in vivo* applications of theranostic nanostructures in the brain. Nanomedicine. 2014: 10: 851-858.
47. Kundrotas G, Karabanovas V, Pleckaitis M, et al. Uptake and distribution of carboxylated quantum dots in human mesenchymal stem cells: cell growing density matters. J Nanobiotechnology. 2019: 17: 39.
48. Takeuchi Y, Suzuki H, Sasahara H, et al. Encapsulation of iron oxide nanoparticles into red blood cells as a potential contrast agent for magnetic particle imaging. Adv Biom Eng. 2014: 3: 37-43.
49. Kapur A, Medina S, Wang W, et al. Enhanced Uptake of Luminescent Quantum Dots by Live Cells Mediated by a Membrane-Active Peptide. ACS Omega. 2018: 3: 17164−17172.
50. Tatiana Galochkina, Matthieu Ng Fuk Chong, Lylia Challali, et al. New insights into GluT1 mechanics during glucose transfer. Sci Rep. 2019: 9: 998.